

Article

## Remote-Sensed Monitoring of Dominant Plant Species Distribution and Dynamics at Jiuduansha Wetland in Shanghai, China

Wenpeng Lin <sup>1</sup>, Guangsheng Chen <sup>2,\*</sup>, Pupu Guo <sup>1</sup>, Wenquan Zhu <sup>3</sup> and Donghai Zhang <sup>3</sup>

<sup>1</sup> College of Tourism, Shanghai Normal University, Shanghai 200234, China;  
E-Mails: linwenpeng@163.com (W.L.); ppdzn0613@126.com (P.G.)

<sup>2</sup> Environmental Sciences Division, Oak Ridge National Laboratory, TN 37830, USA

<sup>3</sup> College of Resource, Beijing Normal University, Beijing 100875, China;  
E-Mails: zhuwq75@bnu.edu.cn (W.Z.); donghai\_zhang@mail.bnu.edu.cn (D.Z.)

\* Author to whom correspondence should be addressed; E-Mail: cheng@ornl.gov;  
Tel.: +1-865-576-2006; Fax: +1-865-241-4088.

Academic Editors: Parth Sarathi Roy and Prasad S. Thenkabail

Received: 10 June 2015 / Accepted: 31 July 2015 / Published: 11 August 2015

---

**Abstract:** *Spartina alterniflora* is one of the most hazardous invasive plant species in China. Monitoring the changes in dominant plant species can help identify the invasion mechanisms of *S. alterniflora*, thereby providing scientific guidelines on managing or controlling the spreading of this invasive species at Jiuduansha Wetland in Shanghai, China. However, because of the complex terrain and the inaccessibility of tidal wetlands, it is very difficult to conduct field experiments on a large scale in this wetland. Hence, remote sensing plays an important role in monitoring the dynamics of plant species and its distribution on both spatial and temporal scales. In this study, based on multi-spectral and high resolution (<10 m) remote sensing images and field observational data, we analyzed spectral characteristics of four dominant plant species at different green-up phenophases. Based on the difference in spectral characteristics, a decision tree classification was built for identifying the distribution of these plant species. The results indicated that the overall classification accuracy for plant species was 87.17%, and the Kappa Coefficient was 0.81, implying that our classification method could effectively identify the four plant species. We found that the area of *Phragmites australis* showed an increasing trend from 1997 to 2004 and from 2004 to 2012, with an annual spreading rate of 33.77% and 31.92%, respectively. The area of *Scirpus mariqueter* displayed an increasing trend from 1997 to

2004 (12.16% per year) and a decreasing trend from 2004 to 2012 (−7.05% per year). *S. alterniflora* has the biggest area (3302.20 ha) as compared to other species, accounting for 51% of total vegetated area at the study region in 2012. It showed an increasing trend from 1997 to 2004 and from 2004 to 2012, with an annual spreading rate of 130.63% and 28.11%, respectively. As a result, the native species *P. australi* was surrounded and the habitats of *S. mariqueter* were occupied by *S. alterniflora*. The high proliferation ability and competitive advantage for *S. alterniflora* inhibited the growth of other plant species and we anticipate a continuous expansion of this invasive species at Jiuduansha Wetland. Effective measures should be taken to control the invasion of *S. alterniflora*.

**Keywords:** decision tree classification; Normalized Difference Vegetation Index (NDVI); phenological characteristics; invasive species

---

## 1. Introduction

Remote sensing has been widely applied to monitor spatial distribution patterns of plant populations owing to the advantages of macroscopic view, speediness, dynamic, and comprehensiveness [1–3]. However, remote sensing data contain a certain amount of uncertainty, such as different objects may have the same spectral features or the same object may have different spectral features [4,5]. Environmental factors may lead to changes of spectral features, especially for the interpretation of a single image. For this reason, some researchers have attempted to use multi-temporal remote sensing images of plants at different phenological stages to interpret vegetation distribution. For example, Tucker *et al.* [6] applied the principal component analysis (PCA) with the Normalized Difference Vegetation Index (NDVI) for dimension reduction to improve the classification accuracy. Li *et al.* [7] used a macroscopic vegetation classification scheme and the seasonal change of NDVI to identify vegetation dynamics in China and proved that their classification method had a good feasibility. Agrawal *et al.* [8] classified vegetation distribution through seasonal variation, reflected by multi-temporal NDVI, and gained a high degree of classification accuracy. These studies suggest that the benchmarking direction for monitoring vegetation dynamics is to interpret multi-temporal remote sensing images at different phenological stages with the help of other supplemental information [9].

Multi-temporal remote sensing images of plants at different phenological stages can help to partially solve the problems that different objects have the same spectral features or the same objects have different spectral features, but it still cannot overcome the problem of mixed pixel spectrums (a pixel contains spectral information of many vegetation types) in low-resolution remote sensing images. Most of the existing data productions of land cover on regional and global scales (such as the DISCover, provided by International Geosphere-Biosphere Programme (IGBP), the GLC2000, released by University of Maryland, or the MODIS land cover quarterly products [10–14]) are obtained from the classification results of low- and medium-resolution remote sensing data (spatial resolution is equal to or more than 30 m) and the classification system generally involves only several types of dominant plants. Furthermore, those productions are widely used in ecological environmental monitoring on large and mesoscales, but they are not suitable for eco-environmental surveys of community succession and plant

invasion on finer scales (e.g., <10 m). In recent years, a large number of high-resolution remote sensor platforms were launched and images were successfully retrieved, which provides a new technology and large amounts of available data for macro quantitative research of dominant plant populations [15,16].

Jiuduansha Wetland in Shanghai, China is a nature reserve with four major plant species, including *Phragmites australis*, *Spartina alterniflora*, *Zizania latifolia* and *Scirpus mariquete*. *S. alterniflora* is one of the 16 most important invasive species which were identified by the Chinese government. This invasive species was first introduced into the Jiuduansha Wetland in the 1990s and spread very fast thereafter. At present, it accounts over 50% of the vegetated area of this wetland. Therefore, monitoring the dynamics of *S. alterniflora* and other dominant plant species at Jiuduansha Wetland can help us have an insight into the invasive mechanisms of *S. alterniflora* [17], thereby providing scientific guidelines to manage or control this invasive species. However, because of the complex characteristics of the river mouth beach wetlands due to its special location between the intertidal zone and sub-tidal zone, where water ebbs and flows and climate alternates with drying and wetting, it is very difficult to conduct a comprehensive field investigation on a large scale [18,19]. The multispectral and high-resolution images from satellites could greatly help monitor vegetation dynamics at Jiuduansha Wetland.

In this study, based on a combination of field investigation data and high-resolution remote sensing images from ZY-1 02C (ZiYuan1) and ZY-3 (ZiYuan3) satellites, we intended to analyze the differences in spectral characteristics of four dominant plant species at different green-up phenophases. A decision tree classification was built for identifying the distribution of dominant plant species. Finally, based on previous research results, we further analyzed the dynamic changes in the dominant plants during 1997–2012 at Jiuduansha Wetland.

## 2. Data and Methods

### 2.1. Study Area

Jiuduansha Wetland is a national nature reserve, which is located in sediment-laden estuary (121°46'~122°15'E, 31°03'~31°17'N) between the northern and the southern troughs of the Yangtze River estuary. It is the farthest alluvial sand bar off the coast of the Yangtze River estuary. This wetland covers four islands: the Jiangyanansha, Shangsha, Zhongsha and Xiasha islands from west to east (Figure 1). Jiuduansha Wetland formed in the 1950s and then kept silting, stretching east and expanding under the interaction between rivers and the ocean. Nowadays, it is the largest original river mouth beach wetland in the Yangtze River estuary. Its area reaches up to 421 km<sup>2</sup> with altitudes above –5 m. The area belongs to the subtropical continental monsoon climate with an annual average temperature of 15.7 °C, 1798 annual sunshine hours, and average annual rainfall of about 1145 mm.

Jiuduansha Wetland is a typical salt marsh ecosystem that has abundant vegetation biomass, simple community structure, and low-level biodiversity. There are only four dominant plant species distributed at Jiuduansha Wetland including *Phragmites australis*, *Spartina alterniflora*, *Scirpus mariquete*, and *Zizania latifolia*. *P. australis* and *S. alterniflora* were introduced in Shangsha Island and Zhongsha Island since 1997. They expanded to form gradient distribution patterns and, as a result, the habitats of the original *S. mariqueter* plants were occupied by them [20,21]. According to long-term monitoring of plant phenophases by the Jiuduansha Wetland Administration, the green-up time of

*S. alterniflora* is in the middle May and the withering period is from December to January of the next year. Green-up time of *Z. latifolia* is the same as *P. australis*, which is in the middle of April. Their withering period is from November to December. *S. mariquete* has a green-up time from late April to early May and a withering period from November to December.

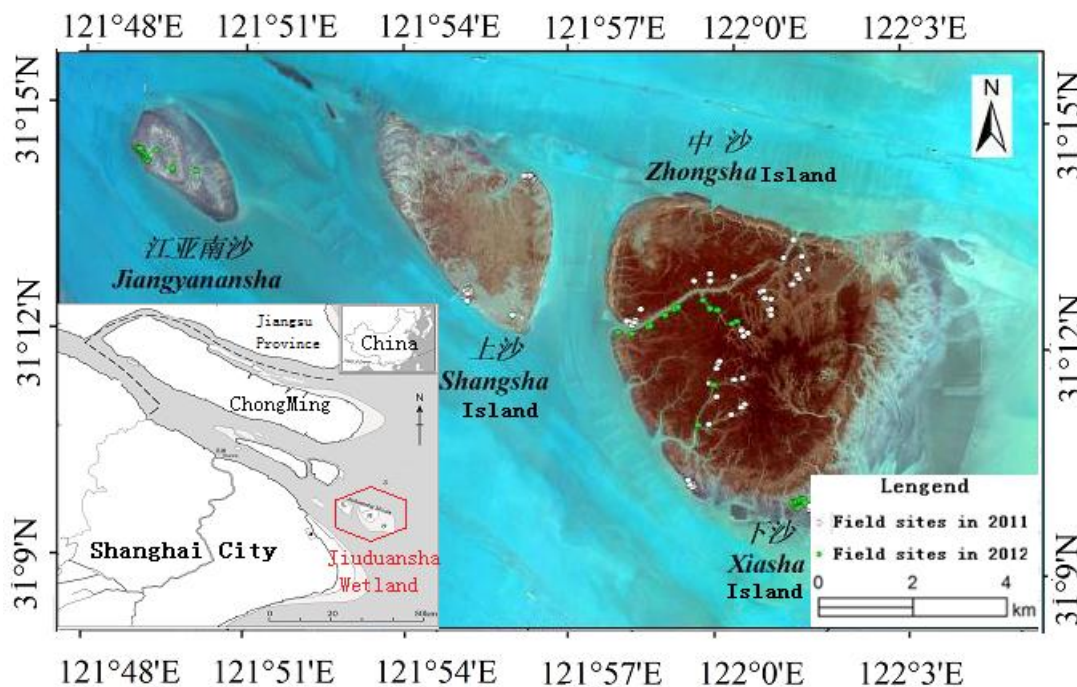


**Figure 1.** The True-color composite image of the study area obtained from ZY-1 02C satellite on 16 May 2012 and the spatial distribution of field observation sites (dotted points).

## 2.2. Data Acquisition and Preprocessing

The ZiYuan1 (ZY-1 02C) and ZiYuan3 (ZY-3) satellites were successfully launched on 22 December 2011 and 9 January 2012, respectively, by the China Centre for Resources Satellite Data and Application (CRSDA) (Table 1). CRSDA has successfully processed the data that were downloaded on the first days from the two satellites and produced remote sensing images. The ZY-1 02C satellite is the first operational satellite customized for land and resource users in China. Onboard the satellite, there are two panchromatic high-resolution cameras with spatial resolution of 2.36 m and a panchromatic multispectral camera with spatial resolution of 5 m and 10 m. The multispectral images acquired by ZY-1 02C include green (0.52–0.59  $\mu\text{m}$ ), red (0.63–0.69  $\mu\text{m}$ ), and near infrared (0.77–0.89  $\mu\text{m}$ ), with a resolution of 10 m. The ZY-3 satellite is the first high-resolution stereo mapping satellite of China. It carries two types of pushbroom imaging sensors for the acquisition of multispectral and panchromatic images. The multispectral images acquired by ZY-3 include blue (0.45–0.52  $\mu\text{m}$ ), green (0.52–0.59  $\mu\text{m}$ ), red (0.63–0.69  $\mu\text{m}$ ) and near infrared (0.77–0.89  $\mu\text{m}$ ) with a resolution of 5.8 m. The panchromatic sensor is composed of three telescopes pointing at forward, backward, and nadir angles. The inclination angles of the forward and backward telescopes are  $\pm 23.5^\circ$  from nadir to realize a base-to-height ratio of 0.87. At present, The data from ZY-3 have been widely applied in dynamic monitoring of land utilization, information-based management of territorial resources, monitoring of

geologic and mineral resources, survey of forest and agricultural resources, survey and monitoring of water resources, and water conservancy projects, urban planning, *etc.*

Some of the characteristics of the two periods of remote sensing images from two satellites were shown in Table 1. The dates for obtaining these images were at low ebb so that they can capture the vegetation near the tidal flat. Before interpretation, we implemented geometric correction, radiation calibration, and atmospheric correction for both images. In particular, geometric correction used field survey GPS points as reference, as well as the 2 m resolution fusion image (correction to 1:50,000 topographic map) of Formosat-2, 2007, and the root square mean error (RSME) is less than 0.5 pixel. Radiation calibration used absolute radiation calibration coefficient as reference offered by the China Centre for Resources Satellite Data and Application (<http://www.cresda.com/n16/n1115/n1522/n2103/index.htm>). We found that radiation correction can increase the difference of NDVI values and make it easier for interpreting various plant species. The ENVI FLAASH module was applied in atmospheric correction ([http://www.exelisvis.com/portals/0/pdfs/envi/Flaash\\_Module.pdf](http://www.exelisvis.com/portals/0/pdfs/envi/Flaash_Module.pdf)).

**Table 1.** The characteristics of selected remote sensing images.

Sensor	Acquisition Date	Band	Resolution (m)	Tidal Level	Application
ZY-1 02C Satellite	2012.05.16	multi-spectral	10	low	automatic identification of vegetation type
		Panchromatic band	5	low	auxiliary visual interpretation
ZY-3 Satellite	2012.03.25	multi-spectral	5.8	low	automatic identification of vegetation type

We conducted two field investigation campaigns to observe the distributions of four plant species on 25 to 28 October 2011 and 14 and 15 October 2012, respectively. In total, we collected 156 sample points (Figure 1, Table 2). At each sampling point, we recorded the plant species, longitude, and latitude information. In order to avoid the problems of mixed pixel spectrum and reduce the effect of geometric correction error, each sample point mainly had a single plant species and covers an area more than 30 m × 30 m. Since we were not able to access deep inside of the study area, the field investigation sample points were mostly distributed within 200 m of the tidal creek. Correspondingly, we also identified 156 pixels (10 m × 10 m), which are located within the field observational sites, from the classified satellite images. Since the field observation sites cover an area  $\geq 30 \text{ m} \times 30 \text{ m}$ , the pixels matched very well with the field observation sites. In addition, we also used ENVI4.8 classification accuracy evaluation module to randomly generate an additional 148 sample points from the satellite images that distributed evenly in the study area (Table 2). We then conducted a visual interpretation to identify the dominant plant species in these pixels and to evaluate the classification accuracy based on our classification method (see Section 2.4).

**Table 2.** The leaf-on and leaf-off phenophases of different plant species and sampling numbers from field investigation and satellite images

Plant Species	Leaf-on Time	Leaf-off Time	Field Sample Numbers		Selected Pixels from Satellite Images
			2011	2012	
<i>P. australis</i>	Mid-April	November	42	14	108
<i>S. alterniflora</i>	Mid-May	December	32	21	124
<i>Z. latifolia</i>	Mid-April	November	0	13	18
<i>S. mariqueter</i>	Late-April	November	26	8	54
Total			100	56	304

### 2.3. Spectral Characteristics of Different Plant Species

According to the field observation data and visual interpretations of satellite images, we found that the four dominant plants have obvious differences in the green-up timing; therefore, we selected 15 sample points for each plant species to identify their spectral characteristics. By retrieving the reflectivity of the green, red, and near infrared bands from the images of two periods, we calculated the average reflectance and NDVI values of the four plant species at each band and constructed a spectral knowledge base for contrastive analysis (Table 3).

After combination of the near infrared band, red band, and green band, the areas with high vegetation coverage displayed a dark red color, areas with moderate vegetation coverage displayed a bright red color, and areas with low vegetation coverage displayed a brown or dark yellow color. On 25 March 2012, the dominant plant species had not fully greened up yet (Figure 1A), the areas with *S. alterniflora* distribution generally displayed a reddish brown color (combined reflectance of 0.075, 0.082, and 0.11 at green, red, and infrared bands, respectively) which is distinct from the light brown color (combined reflectance of 0.10, 0.12, and 0.15 at green, red, and infrared bands, respectively) at the areas with *P. australis* distribution. However, it was difficult to differentiate *Z. latifolia* (combined reflectance of 0.12, 0.12, and 0.13 at green, red, and infrared bands, respectively) from *S. mariqueter* (combined reflectance of 0.11, 0.13, and 0.14 at green, red, and infrared bands, respectively) because both exhibited a light brown color. On 16 May 2012, *P. australis* has been greened up (Figure 1A) and displayed a bright red color (combined reflectance of 0.11, 0.085, and 0.25 at green, red, and infrared bands, respectively). *P. australis* was widely distributed in the Zhongxia and Xiasha Islands, and close to the distribution area of *S. alterniflora*, which displayed as a reddish brown color in image (combined reflectance of 0.101, 0.091, and 0.14 at green, red, and infrared bands, respectively). *Z. latifolia* was widely distributed in Jiangyanansha Island and had a similar bright red color (combined reflectance of 0.12, 0.093, and 0.22 at green, red, and infrared bands, respectively) with *P. australis*. The *S. mariqueter* displayed the similar color with *S. alterniflora* (combined reflectances of 0.11, 0.10, and 0.15 at green, red, and infrared bands, respectively), but with a finer texture.

As shown in Table 3, plants on May 16 could be divided into two groups according to NDVI values. *S. alterniflora* and *S. mariqueter* had a NDVI greater than 0.4 and *P. australis* and *Z. latifolia* had a NDVI of about 0.2. The two plants in each group had similar spectra and were distributed in adjacent locations, so it was difficult to distinguish them simply based on NDVI values using a single phase multispectral image. On 25 March plant reflectance of green, red, and near infrared bands displayed a

gradual increasing trend as compared to that from 16 May. Except for *S. alterniflora*, the reflectance of the other three species was intertwined and their domains were similar, so it was difficult to distinguish them simply using a single phase multispectral image. The NDVI values for *S. mariqueter* and *Z. latifolia* were quite similar hence increased the difficulty to distinguish them.

**Table 3.** The spectral reflectance (magnified by 10,000 times) of the four dominant plant species at Jiuduansha Wetland during two time periods.

Plant Species	2012-03-25					2012-05-16				
	Image	Spectral Reflectance			NDVI	Image	Spectral Reflectance			NDVI
		Green	Red	Near Infrared			Green	Red	Near Infrared	
<i>P. australis</i>		1041.41	1188.74	1480.74	0.11		1108.90	848.58	2473.68	0.49
<i>S. alterniflora</i>		752.16	820.56	1108.46	0.15		1028.20	906.87	1376.87	0.21
<i>Z. latifolia</i>		1153.06	1195.89	1316.67	0.05		1156.88	925.29	2240.35	0.42
<i>S. mariqueter</i>		1145.07	1264.00	1438.11	0.06		1124.75	1003.39	1479.25	0.19

#### 2.4. Schemes for Identifying Dominant Plant Species

We used the two phases of multi-spectral satellite images to retrieve NDVI (Figure 2). It could be seen that water ( $NDVI < 0$ ), bare ground, and vegetation could be distinguished well in terms of NDVI. NDVI in May (hereinafter referred to NDVI5) could be grouped into two categories (Figure 2B; Table 3): the high value area (dominant species are *S. alterniflora* and *S. mariqueter*) and low value area (dominant species are *P. australis* and *Z. latifolia*). NDVI in March (hereinafter referred to NDVI3) could be used to differentiate the vegetated area and non-vegetated area, but the difference among plant species was not obvious, so it was hard to identify them. For this reason, we linearly stretched the red and near-infrared bands to the range of 0–255 and then recalculated NDVI (hereinafter referred to NDVI3-S). As a result, the difference of NDVI was enhanced after stretching and it was easier to distinguish three groups of dominant plant species: *S. alterniflora*, *P. australis*, and the other two species.

Through the analysis of the differences in spectral characteristics and green-up timing of the four dominant plants, we found that *P. australis* and *Z. latifolia* had similar spectral characteristics in visible and near infrared bands in May, so it was hard to distinguish them using a single phase multispectral image. Howeverm they had different green-up timing, so we could divide *P. australis* and *Z. latifolia* based on the difference of NDVI between March and May. In March, *S. mariqueter* and *Z. latifolia* had similar NDVI but in May the NDVI of *Z. latifolia* was significantly higher than that of *S. mariqueter*, so we could execute an intersection operation at the mixed areas of *S. mariqueter* and *Z. latifolia* to limit the distribution range of these two species. In addition, *Z. latifolia* only exists in Jaingyanansha Island based on our field investigation. Thus, the areas with high NDVI values in Shangsha Island, Zhongxia Island, and Xiasha Island could be identified as *P. australis*.

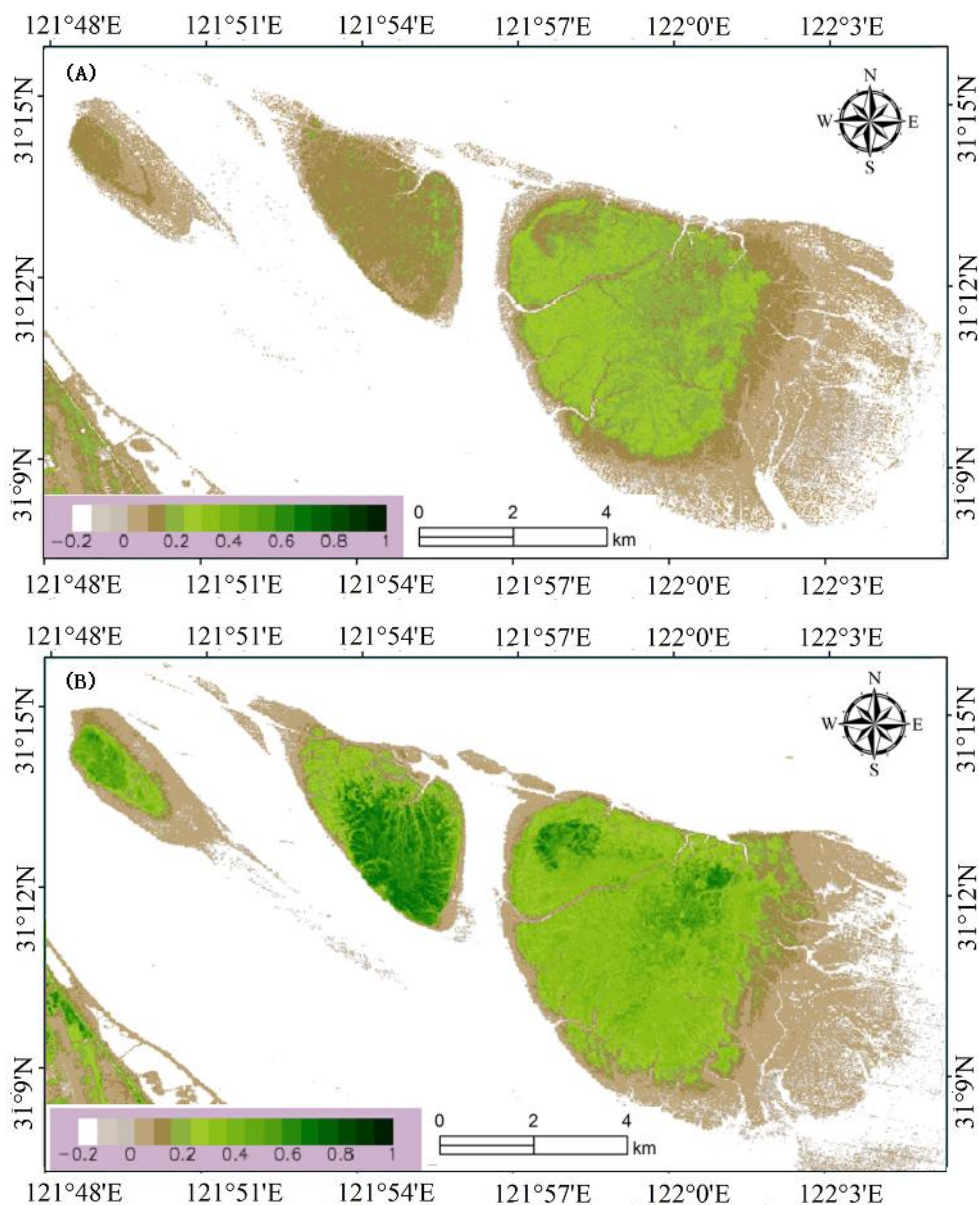


**Figure 2.** The NDVI values at Jiuduansha Wetland in 2012: (A) The NDVI on 25 March 2012; (B) the NDVI on 16 May 2012.

Based on the analysis above, we built a decision tree for classification in ENVI4.8 software for identifying the distribution of the four dominant plant species in the study area. The specific technical procedures were listed as follows (Figure 3):

- (1) Set NDVI5 as the object and assigned 0.12 as a threshold to divide NDVI5 into vegetated area ( $\text{NDVI5} > 0.12$ ) and non-vegetated area ( $\text{NDVI5} \leq 0.12$ ).
- (2) Assigned  $-0.1$  as a threshold to identify non-vegetated areas and water and assigned 0.28 as a threshold to group the vegetation areas into NDVI5-low and NDVI5-high areas.
- (3) According to the difference in green-up time, we identified the areas with NDVI5-low where  $\text{NDVI3-S} > -0.06$  were *S. alterniflora* and the areas where  $\text{NDVI3-S} \leq -0.06$  were *S. mariqueter*. We identified the areas with NDVI5-high where  $\text{NDVI3} > -0.06$  was *P. australis* and the areas with  $\text{NDVI3} \leq -0.06$  was *Z. Latifolia*.

Since *Z. latifolia* was only distributed on the Jiangyanansha Island and difficult to differentiate from *P. australis* based on phenophases, we individually treated it during classification. Firstly, Jiangyanansha Island was cut out to make the decision tree classification. Secondly, we modified the NDVI-high to *P. australis* in the classification decision tree at the rest of islands. Finally, we mosaicked the two classification results and obtained the final vegetation classification result.

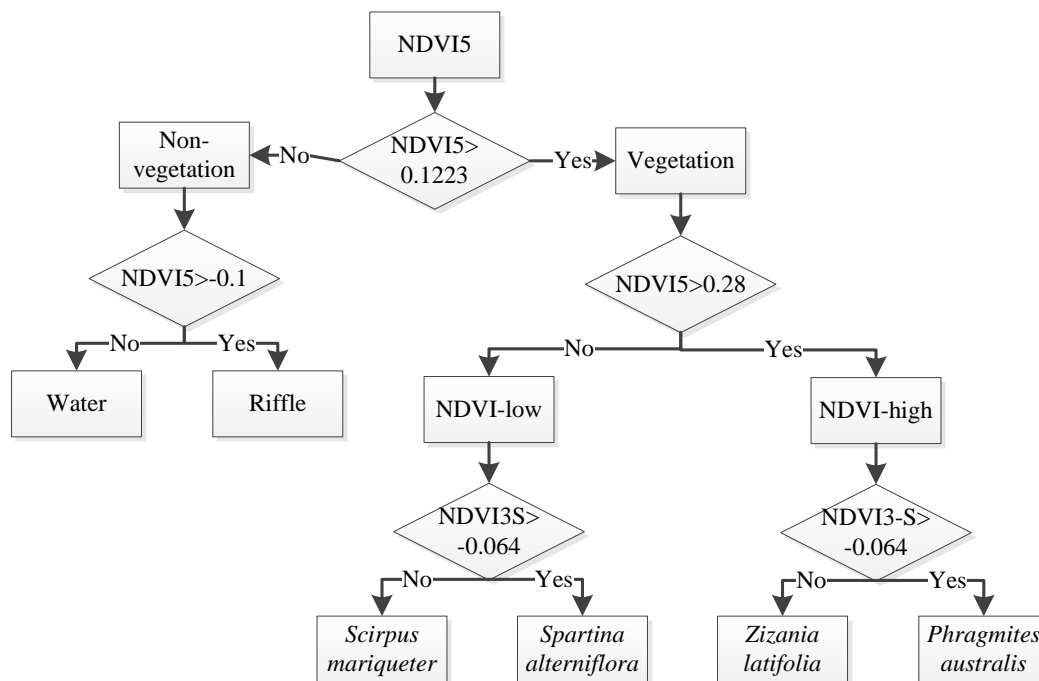


**Figure 3.** The classification decision tree for dominant plant species. NDVI5: NDVI in May; Non-vegetation: non-vegetated area; Vegetation: vegetated area; NDVI5-low: low NDVI value in May; NDVI5-high: high NDVI value in May; NDVI3-S: NDVI in March.

### 3. Results and Analysis

#### 3.1. Classification Precision Evaluation

The classification results of dominant plants at Jiuduansha Wetland are shown in Figure 4. We compared the plant species based on field investigation with those based on classified images (Table 4). According to the relationships between classification accuracy and Kappa coefficient [22], it implies good classification accuracy when Kappa coefficient is between 0.6 to 0.8, while it indicates the classification accuracy is perfect when Kappa coefficient is between 0.8 and 1.0. We found that the overall classification precision was 87.17% and kappa coefficient was 0.81. The precision for *S. alterniflora* and *P. australis* was relatively higher. There were some misclassifications between *P. australis* and *S. alterniflora*, and between *P. australis* and *Z. latifolia*. Moreover, few pixels with *S. mariqueter* were classified as *P. australis* and *S. alterniflora*. Most of the errors were resulted from the mixture of multiple plant species in a single pixel at 10 m resolution.

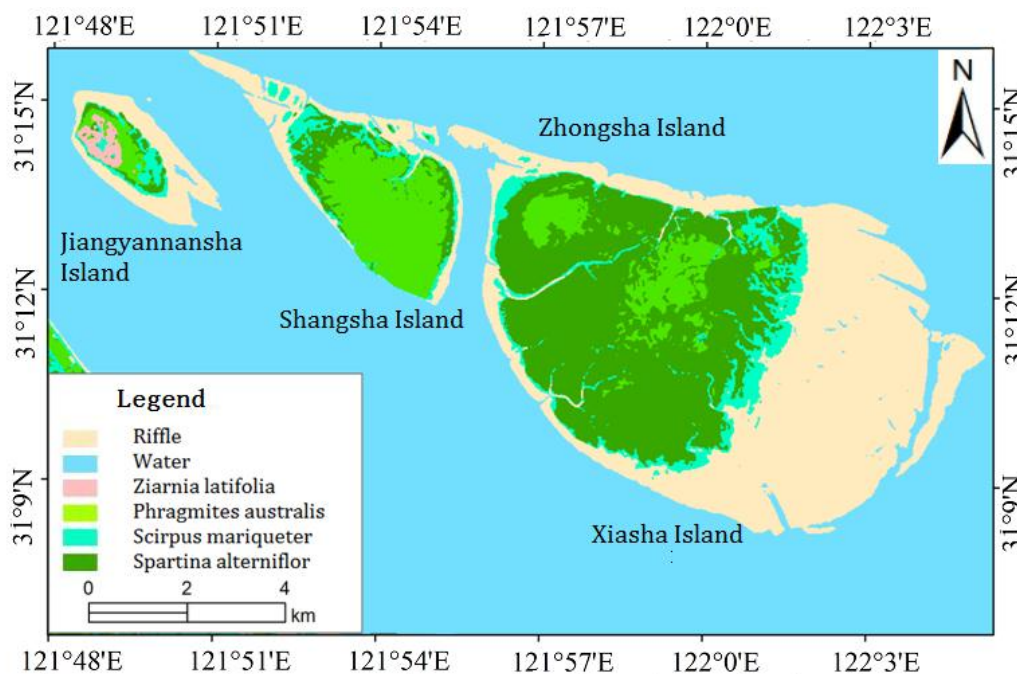


**Figure 4.** The classified distribution of dominant plant species at Jiuduansha Wetland in 2012.

**Table 4.** The precision evaluations for the decision tree classification results.

Plant species	Reference Pixel Number	Classified Pixel Number	Correct Number	Production Precision	User Precision
<i>S. mariqueter</i>	54	59	45	0.83	0.76
<i>S. alterniflora</i>	124	130	112	0.90	0.86
<i>P. australi</i>	108	98	93	0.86	0.95
<i>Z. latifolia</i>	18	17	15	0.83	0.88
Total reference pixel number	304	304	265		
Overall classified precision = 87.17%					
Kappa coefficient = 0.81					

### 3.2. Spatial Distribution of Plant Species

Figure 4 showed the spatial distribution patterns of four plant species based on the two time periods of NDVI images in 2012. Table 5 listed the distribution area of four dominant plant species on each island in 2012. Specifically, *P. australis* accounted for 31.33% of the total vegetation area in the study area and distributed on all four islands. The largest area (1089.46 ha) of *P. australis* was distributed on Shangsha Island, followed by Xiasha Island and Zhongsha Island, and the least was Jiangyanansha Island. *P. australis* generally grows on the high- or middle-level tidal flats with relatively high elevation (>2.9 m). With increasing elevation, this species can turn from a spotty distribution to form a clustered single plant community. *S. alterniflora* could form a large area of a single dominant salt marsh plant community at Jiuduansha Wetland. It has wide adaptive amplitude that its upper limit of distribution can reach the *P. australis* community and lower limit of distribution can reach the *S. mariqueter* community. The distribution area of *S. alterniflora* was the largest as compared to other species at Jiuduansha Wetland, which accounted for 51.33% of the total vegetated land area. *S. alterniflora* was mostly distributed on Xiasha Island (2491.49 ha), followed by Zhangsha Island

(751.31 ha), while only a small area distributed on other two islands; The area of *S. mariqueter* was the smallest as compared to other three dominant plant species at Jiuduansha Wetland and accounted for 13.82% of the total vegetated area. It mainly distributed on Shangsha Island (303.51 ha) and Xiasha Island (433.22 ha). Most of *S. mariqueter* grows on middle tidal flats where elevation is about 2–3 m, whose community density increased with elevation. *Z. latifolia* was mainly distributed on Jiangyanansha Island. It covered an area of 225.22 ha and occupied about 60% of the land area.

**Table 5.** The area (ha) of the four dominant plant species on different islands of Jiuduansha Wetland in 2012.

Islands	<i>P. australis</i>	<i>S. alterniflora</i>	<i>S. mariqueter</i>	<i>Z. latifolia</i>	Total
Jiangyanansha	12.66	6.93	109.11	225.22	353.93
Shangsha Island	1089.46	52.47	303.51	0.00	1445.43
Zhongsha Island	258.37	751.31	42.99	0.00	1052.67
Xiasha Island	654.46	2491.49	433.22	0.00	3579.17
Total	2014.95	3302.20	888.83	225.22	6431.19
Percentage	31.33	51.35	13.82	3.50	100.00

### 3.3. Temporal Changes in Plant Species

Based on Landsat TM/ETM<sup>+</sup> images and field investigation data, Huang and Zhang [23] estimated the area and spatial distribution of three plant species (*i.e.*, *S. alterniflora*, *P. australis*, and *S. mariqueter*) at the study area. Based on these previous data, we compared the area and spatial pattern of these dominant plant species in 1997, 2004, and 2012 at Jiuduansha Wetland (Table 6). The results indicated that *S. alterniflora*, an invasive plant species, has experienced a process of invasion, settlement, and stabilization from 1997 to 2004. The wide ecological amplitude and high proliferation capability make it easier to occupy the favorable habitats. It can survive in the northern Zhongsha Island and the central Xiasha Island with an annual spreading rate of 130.63% from 1997 to 2004. *P. australis*, as a native plant species that mainly distributes in the southern Shangsha Island and the northern Zhongsha Island, expanded rapidly with an annual spreading rate of 33.77% due to human disturbance. *S. mariqueter* is a pioneer community on tidal flat in this region. Its emergence and growth created space for *S. alterniflora* and *P. australis* to settle and spread. Part of its habitat was occupied by other species but the bare sandy land at the peripheral island provided new habitat for it, making the area of *S. mariqueter* maintain an annual spreading rate of 12.16%. However, on a spatial scale, the expansion radius of *S. alterniflora* and *P. australis* on Zhongsha Island and Xiasha Island is significantly larger than the bare sandy land, which resulted in a decreasing tendency for the available living space of *S. mariqueter*.

From 2004 to 2012, *S. alterniflora* and *P. australis* had already become the dominant plant species at Jiuduansha Wetland through continuous spreading. *P. australis* maintained an annual spreading rate of 31.92%, which was significantly lower than that during 1997–2004. The expansion area of *P. australis* was mainly distributed on the southern Shangsha Island, where it grew rapidly without the competition of *S. alterniflora*. However, due to the faster expansion rate of *S. alterniflora*, *P. australis* on Zhongsha Island and Xiasha Island shifted from a scattered distribution pattern into a continuous patch distribution pattern without an obvious increase in distribution boundary. *S. alterniflora*

expanded rapidly with an annual spreading rate of 28.11% from 2004 to 2012. After a fast invasion from 1997 to 2004, *S. alterniflora* has been stabilized and occupied large area on Zhongsha Island and Xiasha Island. The area of *S. mariqueter* displayed a decreasing trend with an annual rate of 7.05% as a result of the *S. alterniflora* expansion. In addition to the existence of a wide living space on the southwestern Shangsha Island and the eastern Xiasha Island, *S. mariqueter* only had a very narrow distribution area in the vicinity between vegetated and non-vegetated areas.

**Table 6.** The area (ha) and spreading rates (%/yr) of the dominant plant species at Jiuduansha Wetland in 1997, 2004, and 2012 (\*—data are from Huang and Zhang [23]).

Time	<i>P. australis</i>		<i>S. alterniflora</i>		<i>S. mariqueter</i>	
	Area (ha)	Spreading Rate (%/yr)	Area (ha)	Spreading Rate (%/yr)	Area (ha)	Spreading Rate (%/yr)
1997 *	167.5		100		966.56	
2004 *	563.49	33.77	1014.39	130.63	1789.02	12.16
2012	2002.29	31.92	3295.26	28.11	779.72	-7.05

The spreading rate of *S. alterniflora* was much higher than that of *P. australis* in the recent eight years (2004–2012). Meanwhile, *S. alterniflora* tended to occupy the distribution area of the *S. mariqueter* on Zhongsha Island and Xiasha Island. It can be seen that the rapid expansion of the sand bar at Jiuduansha Wetland provided more suitable habitats for *S. alterniflora* to spread and we anticipate a further expansion of this invasive species. In the meanwhile, the high proliferation capability as well as competitive advantage for *S. alterniflora* inhibited the growth of other adjacent plant species at Jiuduansha Wetland and threatened the local native ecosystem stability and biodiversity [24,25]. It is necessary to take some effective measures to control the spreading of *S. alterniflora*.

#### 4. Conclusions

In this study, based on the field investigation data and remote sensing images from the ZY-1 02C and ZY-3 satellites, we analyzed the differences in spectral characteristics of the four dominant plant species at different green-up phenophases and built a decision tree classification to identify the distribution of them at Jiuduansha Wetland. Combining with previous research results, we further analyzed the changes of spatial distribution for the four dominant plant species at Jiuduansha Wetland during 1997–2012. The conclusions were listed as follows:

- (1) Taking advantage of the different characteristics on NDVI of the four dominant plant species at different green-up phenophases, we developed a decision tree classification scheme to identify the distribution of these species. This method could effectively identify the four dominant plant species at Jiuduansha Wetland, with an overall classification accuracy of 87.17% and the Kappa Coefficient of 0.81;
- (2) *S. alternifloras* formed a large area of a single dominant salt marsh plant community which covered an area of 3302.20 ha at Jiuduansha Wetland. It had wide ecological amplitude that its upper limit of distribution can reach *P. australis* zone and lower limit of distribution can reach *S. mariqueter* zone. *P. australis* occupied about 2014.95 ha land area and mainly grew on high and middle tidal flats where elevation is higher than 2.9 m. Most of the *S. mariqueter* plant species

grew on middle tidal flats where elevation is about 2–3 m. It covered an area of 888.83 ha and its community density increased with elevation;

- (3) The area of *P. australis* showed an increasing trend in from 1997 to 2004 and from 2004 to 2012, with an annual spreading rate of 33.77% and 31.92%, respectively. The area of *S. mariqueter* displayed an increasing trend and a decreasing trend from 1997 to 2004 and from 2004 to 2012, respectively, with an annual rate of 12.16% and −7.05%. The area of *S. alterniflora* showed an increasing trend in from 1997 to 2004 and from 2004 to 2012, with an annual spreading rate of 130.63% and 28.11%, respectively. Especially, *S. alterniflora* expanded very quickly and showed a trend of surrounding *P. australis* on Zhongsha Island and Xiasha Island and occupying the habitats of *S. mariqueter*.

Since *S. alterniflora* was introduced into Jiuduansha Wetland, it had successfully settled in this region and eventually became one of the four dominant plant species due to its strong tolerance of salt marsh environment and rapid sexual and asexual reproductive capacity. It expanded rapidly to develop a high density and high productivity single species community under the tidal flats environment. As a result, other plant species in its community had difficulty surviving. Considering its high proliferation ability and competitive advantage, it is time for human intervention to take to control of its spreading; otherwise, the *P. australis* community on Zhongsha Island and Xiasha Island will be threatened and *S. mariqueter* is likely to be replaced. *S. alterniflora* has competitive advantage under the conditions of high salinity and highly flooded frequency while *P. australis* has competitive advantage under the low salinity and low flooded habitat [23], so further observations are needed to determine whether the reducing trend of the *P. australis* community will continue. In addition, the recent vegetation investigation (since 2007) also found another invasive plant species *Solidago canadensis* L. in the Jiuduansha Wetland, which shows an expansion trend due to its high proliferation ability, competitive advantage, and multiple ways of spreading. However, this species displays a plexiform distribution that each of them covers small area (about 1 m<sup>2</sup>), so it is not able to be monitored by remote sensing technology. We will focus on the field survey and analysis of this species in further research in order to provide basic data for research on vegetation dynamics at Jiuduansha Wetland.

## Acknowledgments

This study was supported by the Shanghai Natural Science Foundation (No. 15ZR1431000), National Natural Science Foundation of China (No. 40801168), the Original and Forward-Looking Pre-Research Project of Shanghai Normal University (No. DYL201403), and the National Special Research Fund for Public Welfare (Meteorology) of China (GYHY201406028). We would also like to express our sincere thanks to the anonymous reviewers for their constructive comments.

## Author Contributions

Wenpeng Lin formed the original idea for the study and wrote the original manuscript. Guangsheng Chen offered valuable comments and suggestions to the manuscript and responsible for manuscript revisions. Pupu Guo and Donghai Zhang supervised the process of field campaign and data analysis. Wenquan Zhu provided partial source codes for image analysis and responsible for satellite data collection.

## Conflicts of Interest

The authors declare no conflict of interest.

## References

1. Huang, H.M.; Zhang L.Q.; Yuan, L. The spatio-temporal dynamics of salt marsh vegetation for Chongming Dongtan National Nature Reserve, Shanghai. *Acta Ecol. Sin.* **2007**, *27*, 4166–4172.
2. Roughgarden, J.; Running, S.W.; Matson, P.A. What does remote sensing do for ecology? *Ecology* **1991**, *72*, 1918–1922.
3. Mao, F.; Hou, Y.Y.; Tang, S.J.; Tang, S.H.; Zhang, J.F.; Lu, Z.G. Classification and dynamic changes of grasslands in northern Tibet based on recent 20 years satellite data. *Chin. J. Appl. Ecol.* **2007**, *18*, 1745–1750. (In Chinese with English abstract)
4. Huang, E.X. Research on classification uncertainties of remote sensing image. *Chin. Agric. Sci. Bull.* **2010**, *26*, 322–325.
5. Qi, L.; Zhao, C.J.; Li, C.J.; Li, C.J.; Liu, L.Y.; Tang, C.W.; Huang, W.J. Accuracy of winter wheat identification based on multi-temporal CBERS202 images. *Chin. J. Appl. Ecol.* **2008**, *10*, 2201–2208.
6. Tucker, C.J.; Townshend, J.R.G. African land-cover classification using satellite data. *Science* **1985**, *227*, 227–375.
7. Li, X.B.; Shi, P.J. Research on regulation of NDVI change of Chinese primary vegetation types based on NOAA/AVHRR data. *Acta Bot. Sin.* **1999**, *41*, 88–91.
8. Agrawal, S.; Joshi, P.K.; Shukla, Y.; Roy, P.S. SPOT Vegetation multi temporal data for classifying vegetation in south central Asia. *Curr. Sci.* **2003**, *84*, 1440–1448.
9. Chen, X.Q.; Wang, L.H. Progress in remote sensing phenological research. *Progr. Geogr.* **2009**, *28*, 33–40.
10. Loveland, T.R.; Reed, B.C.; Brown, J.F.; Ohlen, D.O.; Zhu, Z.; Yang, L.; Merchant, J.W. Development of a global land cover characteristics database and IGBP DISCover from 1 km AVHRR data. *Int. J. Remote Sens.* **2000**, *21*, 1303–1330.
11. Hansen, M.C.; Defries, R.S.; Townshend, J.R.; Townshend, R.G.; Sohlberg, R. Global land cover classification at 1 km spatial resolution using a classification tree approach. *Int. J. Remote Sens.* **2000**, *21*, 1331–1364.
12. Bartholomé E.; Belward, A.S. GLC2000: A new approach to global land cover mapping from Earth observation data. *Int. J. Remote Sens.* **2005**, *26*, 1959–1977.
13. Friedl, M.A.; Mciver, D.K.; Hodges, J.C.; Zhang, X.Y.; Muchoney, D.; Strahler, A.H.; Woodcock, C.E.; Gopal, S.; Schneider, A.; Cooper, A.; *et al.* Global land cover mapping from MODIS: Algorithms and early results. *Remote Sens. Environ.* **2002**, *83*, 287–302.
14. Ran, Y.H.; Li, X.; Lu, L. China land cover classification at 1km spatial resolution based on a multi-source data fusion approach. *Adv. Earth Sci.* **2009**, *24*, 192–203.
15. Chen, J.Y.; Tian, Q.J. Vegetation classification based on high-resolution satellite image. *Remote Sens.* **2007**, *11*, 221–227.

16. Chen, R.X.; Wang, C.F. Review on greenland recognition from urban high-resolution satellite image. *Remote Sens. Inf.* **2013**, *28*, 119–125.
17. Wang, Q.; An, S.Q.; Ma, Z.J.; Zhao, B.; Chen, J.K.; Li, B. Invasive *Spartina alterniflora*: Biology, ecology and management. *Acta Phytotaxon. Sin.* **2005**, *44*, 559–588.
18. Shen, F.; Zhou, Y.X.; Zhang, J.; Wu, J.P.; Yang, S.L. Remote-sensing analysis on spatial-temporal variation in vegetation on Jiuduansha wetland. *Oceanol. Limnol. Sin.* **2006**, *37*, 498–504.
19. Li, D.K.; Guo, N. Classifying types of vegetation remote sensing based on growing law in Shaanxi province. *Plateau Meteorol.* **2008**, *27*, 215–221.
20. Jia, J.W.; Wang, L.; Tang, Y.S.; Li, Y.L.; Zhang, W.Q.; Wang, H.L.; Fu, X.H.; Le, Y.Q. Variability in and factors influencing soil microbial respiration in the Jiuduansha wetland under different successional stages. *Acta Ecol. Sin.* **2010**, *30*, 4529–4538.
21. Liu, Y.; Li, X.G.; Yan, Z.Z.; Chen, X.Z.; He, Y.L.; Guo, W.Y.; Sun, P.Y. Biomass and carbon storage of *Phragmites australis* and *Spartina alterniflora* in Jiudian Shoal Wetland of Yangtze Estuary, East China. *Chin. J. Appl. Ecol.* **2013**, *24*, 2129–2134.
22. Landis, J.R.; Koch, G.G. The measurement of observer agreement for categorical data. *Biometrics* **1977**, *33*, 159–174.
23. Huang, H.M.; Zhang, L.Q. Remote sensing analysis of range expansion of *Spartina Alterniflora* at Jiuduansha Shoals in Shanghai, China. *J. Plant Ecol.* **2007**, *31*, 75–82.
24. Gao, H.; Peng, X.W.; Li, B.; Wu, Q.H.; Dong, H.Q. Effects of the invasive plant *Spartina alterniflora* on insect diversity in Jiuduansha wetlands in the Yangtze River Estuary. *Biodivers. Sci.* **2006**, *15*, 400–409.
25. Chen, X.Z. Insect diversity and its influencing factors in Jiuduansha wetland national nature reserve, Shanghai. *J. Shanghai Normal Univ. (Natural Sci.)* **2012**, *41*, 399–409.

© 2015 by the authors; licensee MDPI, Basel, Switzerland. This article is an open access article distributed under the terms and conditions of the Creative Commons Attribution license (<http://creativecommons.org/licenses/by/4.0/>).